ISSN 0015-4628, Fluid Dynamics, 2016, Vol. 51, No. 6, pp. 821–833. © Pleiades Publishing, Ltd., 2016.
Original Russian Text © S.A. Bochkarev, S.V. Lekomtsev, V.P. Matveenko, 2016, published in Izvestiya Rossiiskoi Akademii Nauk, Mekhanika Zhidkosti i Gaza, 2016, Vol. 51, No. 6, pp. 108–120.

Hydroelastic Stability of a Rectangular Plate Interacting with a Layer of Ideal Flowing Fluid

S. A. Bochkarev*, S. V. Lekomtsev, and V. P. Matveenko*****

Institute of Continuous Media Mechanics, Ural Branch of the Russian Academy of Sciences, ul. Akad. Koroleva 1, Perm, 614013 Russia

*e-mail: *bochkarev@icmm.ru, **lekomtsev@icmm.ru, ***mvp@icmm.ru*

Received September 15, 2015

Abstract—The three-dimensional formulation of the problem on the natural vibrations and stability of an elastic plate which interacts with a quiescent or flowing fluid is represented and a finite element algorithm of its numerical implementation is proposed. The governing equations, which describe vortex-free ideal fluid dynamics in the case of small perturbations, are written in terms of the perturbation velocity potential and transformed using the Bubnov–Galerkin method. The plate strains are determined on the basis of the Timoshenko theory. The variational principle of virtual displacements which takes into account the work done by inertial forces and the hydrodynamic pressure is used for the mathematical formulation of the dynamic problem of elastic structure. The solution of the problem is reduced to calculations and an analysis of complex eigenvalues of a coupled system of two equations. The effect of the fluid layer height on the eigenfrequencies and the critical velocities of the loss of stability is estimated numerically. It is shown that there exist different types of instability determined by combinations of the kinematic boundary conditions prescribed at the plate edges.

Keywords: potential fluid, rectangular plate, natural vibrations, hydroelastic stability, boundary conditions, finite element method.

DOI: 10.1134/S0015462816060132

The interaction between elastic plates and gas or liquid is already analyzed over a half-century using various methods including the numerical ones [1, 2]. Considerable part of the investigations is devoted to natural vibrations of the structures interacting with quiescent fluid. The corresponding models are successfully implemented in commercial finite element software packages and envelope a fairly wide class of the problems.

It is well known [2] that an elastic plate located in an axial stream of a liquid or gaseous medium can lose stability when the flow velocity becomes higher than a certain value called the critical velocity. The type of instability, namely, static (divergence) or dynamic (flutter), depends on both the boundary conditions imposed at the plate edges and the flow velocity. In particular, simply supported and rigidly restrained plates lose stability in the form of divergence in the subsonic gas stream and in the form of flutter in the supersonic stream. The plate restrained at one edge and free at the others has the flutter instability in the subsonic stream and the divergent instability in the supersonic stream [3]. Many studies restricted to an analysis of the behavior of plates infinite in all [4–8] or a single [9–13] of the directions are devoted to studying this phenomenon using numerically-analytic methods. In the latter case the fluid flow is assumed to be two-dimensional and, as a rule, the plate is considered as a beam. This assumption is based on experimental investigations of the phenomenon of aeroelastic flutter which showed that the deflection of a cantilever plate under self-exited vibrations depend only slightly on the transverse coordinate. We note that in all the studies mentioned above the excess pressure on the elastic surface from the flowing medium was calculated within the framework of potential theory.

In investigating finite plates [14–19], the main attention was focused on the possibility of generalization of the approaches developed for one-dimensional plates, the estimate of legitimacy of the obtained conclusions on the higher velocities of the loss of stability in the case of plates infinite in one of the directions as compared with finite plates, and an analysis of additional boundary conditions for fluid at the leading or rear edges of cantilevered restrained plates for describing the wake. Some results of these investigations were generalized in [19]. It was found that the stability increases as the plate width decreases. It was noted that various approaches to taking additional boundary conditions for fluid into account lead to the same critical velocities of the flutter, therefore, their effect can be called insignificant.

As distinct from the above-mentioned studies on the interaction of an elastic body with a fluid flow in unbounded space, in [20–22] stability of plates located in a channel with rigid walls was analyzed. In [20] it was shown for a one-dimensional plate (beam) with various boundary conditions that the critical velocity of the loss of stability tends to an asymptotic dependence when the ratio of the channel height to the plate length reaches a certain value. Instability of a plate in the channel with flowing viscous fluid described by the Navier–Stokes equations was considered in [23, 24].

In [24] the development of flutter was demonstrated in the case of joint flow in the upper and lower channels and the development of divergence for flow only in one channel. In the context of results of [24], in [21] it was noted that in the case of fairly small Reynolds numbers the boundaries of stability for short flexible plates are in well agreement with the results obtained within the framework of the potential theory.

In practice, the real structures with complex variants of fastening are frequently subjected to the action of arbitrary distributed loads and, as a result, various types of spatial vibrations and instability can be observed.

The three-dimensional formulation of the problem of hydroelastic stability of plates and its solution by means of the finite element method were given in [25]. The effect of several variants of the kinematic boundary conditions imposed at the plate edges on the boundary of stability was analyzed. However, certain results obtained are not in the qualitative agreement with the well-known numerically-analytic solutions and full-scale observations. Because of the absence of sufficient information in [25] (boundary conditions for fluid, physico-mechanical parameters of the system considered, stability criterion, etc.), the data presented in [25] cannot be reproduced.

The aim of the present study is to create the method of calculation of the natural frequencies, the forms of vibrations, and the boundaries of hydroelastic stability of three-dimensional plates interacting with the layer of a flowing ideal fluid. A parametric analysis of certain characteristics of the system under consideration is carried out to demonstrate the possibilities of the numerical algorithm developed. The effect of the kinematic boundary conditions and the fluid layer height on the form of the loss of stability and the critical velocities of fluid flow is analyzed.

1. MATHEMATICAL FORMULATION OF THE PROBLEM

We will consider a rectangular plate of thickness h located on the top of a channel with rigid walls inside of which a fluid flows with a velocity U. In Fig. 1 we have reproduced the geometric parameters of the model. The strains developed in the plate as a result of the hydrodynamic impact are small. The effect of the boundary layer and the fluid viscosity is neglected.

We will consider irrotational flow of an ideal compressible fluid in terms of the velocity potential $\Phi = Ux + \phi$, where U is the flow velocity, ϕ is the potential of perturbed velocities, and (x, y, z) are the Cartesian coordinates.

In the disturbed state the components of the fluid velocity vector can be determined as follows:

$$v_x = \frac{\partial \Phi}{\partial x} = U + \frac{\partial \phi}{\partial x}, \qquad v_y = \frac{\partial \Phi}{\partial y} = \frac{\partial \phi}{\partial y}, \qquad v_z = \frac{\partial \Phi}{\partial z} = \frac{\partial \phi}{\partial z}. \tag{1.1}$$

In the case of small perturbations the governing equations which describe fluid dynamics in the volume V_f can be written in the coordinate system moving with the plate by means of the perturbation velocity

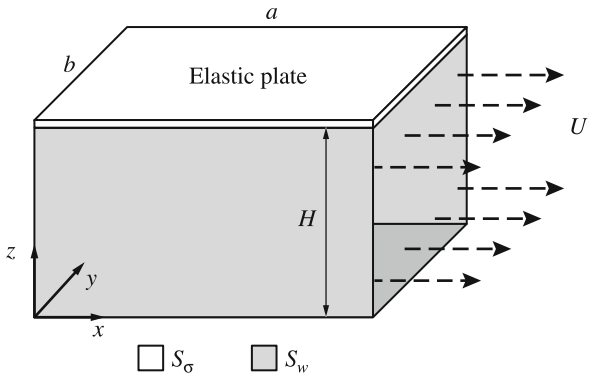

Fig. 1. Computational scheme.

potential ϕ [26]

$$\nabla^2\phi = \frac{1}{c^2}\frac{\partial^2\phi}{\partial t^2} + \frac{2U}{c^2}\frac{\partial^2\phi}{\partial t\partial x} + \mathrm{M}^2\frac{\partial^2\phi}{\partial x^2}. \tag{1.2}$$

Here, c is the speed of sound in fluid and $\mathrm{M} = U/c$ is the Mach number.

On the interface S_σ between the elastic structure and the fluid we impose the condition of equality of the normal stresses and velocities [27]

$$\dot{w} = v_n, \qquad \sigma_{nn}^p = \sigma_{nn}^f, \tag{1.3}$$

where w is the normal component of the plate displacement vector, v_n is the fluid velocity in the direction of the normal to the plane S_σ, and σ_{nn}^p and σ_{nn}^f are the normal stresses of the elastic structure and the fluid on the contact boundary. For small displacements the normal vector to the surface S_σ deviates only slightly from the coordinate z; therefore, within the framework of theory of plates the boundary conditions (1.3) take the form:

$$\left(\frac{\partial w}{\partial t} + U\frac{\partial w}{\partial x}\right) = \frac{\partial\phi}{\partial z}, \tag{1.4}$$

$$p_w = -\rho_f\left(\frac{\partial\phi}{\partial t} + U\frac{\partial\phi}{\partial x}\right). \tag{1.5}$$

The expression (1.4) represents the impermeability condition and (1.5) is the linearized Bernoulli equation, where ρ_f is the fluid density.

On the boundary between the fluid and the rigid wall S_w we impose the condition

$$\frac{\partial\phi}{\partial n} = 0. \tag{1.6}$$

We will assume that there are no perturbations of the longitudinal velocity component at the channel inlet ($x = 0$), then from (1.1) we obtain

$$v_x = U \Rightarrow \frac{\partial\phi}{\partial x} = 0. \tag{1.7}$$

As an alternative variant, we can use the condition

$$\phi = 0. \tag{1.8}$$

We note that this condition, being mathematically correct, can represent certain difficulties for its physical interpretation.

At the channel outlet ($x = a$) the perturbed pressure vanishes

$$-\rho_f\left(\frac{\partial\phi}{\partial t} + U\frac{\partial\phi}{\partial x}\right) = 0 \Rightarrow \frac{\partial\phi}{\partial x} = -\frac{1}{U}\frac{\partial\phi}{\partial t}. \tag{1.9}$$

In [28] it was noted that in the first approximation a condition, which is equivalent to (1.7) correct to notation, can be used instead of (1.9).

The strains of the elastic plate can be determined on the basis of the Timoshenko theory [29]:

$$\boldsymbol{\varepsilon} = \{\varepsilon_{xx},\ \varepsilon_{yy},\ \gamma_{xy},\ \gamma_{xz},\ \gamma_{yz}\}^{\mathrm{T}} = \tilde{\boldsymbol{\varepsilon}} + z\tilde{\mathbf{k}},$$

$$\tilde{\boldsymbol{\varepsilon}} = \{\varepsilon^0_{xx},\ \varepsilon^0_{yy},\ \varepsilon^0_{xy},\ \gamma^0_{xz},\ \gamma^0_{yz}\}^{\mathrm{T}} = \left\{\frac{\partial u}{\partial x},\ \frac{\partial v}{\partial y},\ \frac{\partial u}{\partial y} + \frac{\partial v}{\partial x},\ \frac{\partial w}{\partial x} + \theta_x,\ \frac{\partial w}{\partial y} + \theta_y\right\}^{\mathrm{T}}, \tag{1.10}$$

$$\tilde{\mathbf{k}} = \{\varepsilon^1_{xx},\ \varepsilon^1_{yy},\ \varepsilon^1_{xy},\ 0,\ 0\}^{\mathrm{T}} = \left\{\frac{\partial \theta_x}{\partial x},\ \frac{\partial \theta_y}{\partial y},\ \frac{\partial \theta_x}{\partial y} + \frac{\partial \theta_y}{\partial x},\ 0,\ 0\right\}^{\mathrm{T}},$$

where $(u,\ v,\ w)$ are the displacements of points of the middle surface in the directions of the corresponding axes of the coordinate system $(x,\ y,\ z)$, and θ_x and θ_y are the angles of turning of the normals about the axes y and x.

The physical relations which connect the stress and moment vector $\mathbf{T}$ with the strain vector $\boldsymbol{\varepsilon}$ can be written in the matrix form:

$$\mathbf{T} = \{N_{xx},\ N_{yy},\ N_{xy},\ M_{xx},\ M_{yy},\ M_{xy},\ Q_x,\ Q_y\}^{\mathrm{T}} = \mathbf{D}\boldsymbol{\varepsilon}. \tag{1.11}$$

For the isotropic material the coefficients entering into the stiffness matrix $\mathbf{D}$ can be determined from the following expressions

$$\begin{Bmatrix} N_{xx} \\ N_{yy} \\ N_{xy} \end{Bmatrix} = \int\limits_{-h/2}^{h/2} \mathbf{Q} \begin{Bmatrix} \varepsilon^0_{xx} \\ \varepsilon^0_{yy} \\ \gamma^0_{xy} \end{Bmatrix} dz, \qquad \begin{Bmatrix} M_{xx} \\ M_{yy} \\ M_{xy} \end{Bmatrix} = \int\limits_{-h/2}^{h/2} \mathbf{Q} \begin{Bmatrix} \varepsilon^1_{xx} \\ \varepsilon^1_{yy} \\ \gamma^1_{xy} \end{Bmatrix} z^2\, dz,$$

$$\begin{Bmatrix} Q_x \\ Q_y \end{Bmatrix} = k_s \int\limits_{-h/2}^{h/2} \begin{bmatrix} Q_{33} & 0 \\ 0 & Q_{33} \end{bmatrix} \begin{Bmatrix} \gamma^0_{xz} \\ \gamma^0_{yz} \end{Bmatrix} dz, \qquad \mathbf{Q} = \begin{bmatrix} Q_{11} & Q_{12} & 0 \\ Q_{12} & Q_{22} & 0 \\ 0 & 0 & Q_{33} \end{bmatrix},$$

$$Q_{11} = Q_{22} = \frac{E}{1-\nu^2}, \qquad Q_{12} = \frac{\nu E}{1-\nu^2}, \qquad Q_{33} = \frac{E}{2(1-\nu)}.$$

Here, $k_s = 5/6$, E is the elasticity modulus, and ν is the Poisson's ratio.

For the mathematical formulation of the problem of plate dynamics we will use the variational principle of virtual displacements in which the Bernoulli equation (1.5) and the work of inertia forces are included. In the matrix form it can be written as follows:

$$\int\limits_{S_s} \delta\boldsymbol{\varepsilon}^{\mathrm{T}}\mathbf{D}\boldsymbol{\varepsilon}\, dS + \int\limits_{V_s} \rho_s \delta\mathbf{d}^{\mathrm{T}}\ddot{\mathbf{d}}\, dV - \int\limits_{S_\sigma} \delta\mathbf{d}^{\mathrm{T}}\mathbf{P}\, dS, \qquad \mathbf{P} = \{0,\ 0,\ p_w,\ 0,\ 0\}^{\mathrm{T}}, \tag{1.12}$$

where $\mathbf{d}$ and $\mathbf{P}$ are the vectors of generalized displacements and surface loads and points denote the derivatives with respect to time.

2. NUMERICAL REALIZATION

The solution of the problem is implemented using the finite element method (FEM). Using the Bubnov–Galerkin method [30], the partial differential equation for the perturbation velocity potential (1.2) together with the boundary conditions (1.6)–(1.8) and the impermeability condition (1.4) are reduced to the system of equations in the matrix form:

$$\left(\mathbf{K}_f + \mathbf{A}^c_f\right)\boldsymbol{\phi} + \mathbf{M}_f\ddot{\boldsymbol{\phi}} + \mathbf{C}^c_f\dot{\boldsymbol{\phi}} - \mathbf{C}_f\dot{\mathbf{w}} - \mathbf{A}_f\mathbf{w} = 0, \tag{2.1}$$

where

$$\mathbf{K}_f = \sum_{m_f} \int_{V_f} \left(\frac{\partial \mathbf{F}^{\mathrm{T}}}{\partial x}\frac{\partial \mathbf{F}}{\partial x} + \frac{\partial \mathbf{F}^{\mathrm{T}}}{\partial y}\frac{\partial \mathbf{F}}{\partial y} + \frac{\partial \mathbf{F}^{\mathrm{T}}}{\partial z}\frac{\partial \mathbf{F}}{\partial z} \right) dV, \qquad \mathbf{M}_f = \sum_{m_f} \int_{V_f} \frac{1}{c^2}\mathbf{F}^{\mathrm{T}}\mathbf{F}\, dV,$$

$$\mathbf{A}_f = \sum_{m_\sigma} \int_{S_\sigma} U\mathbf{F}^{\mathrm{T}}\frac{\partial \mathbf{N}^w}{\partial x}\, dS, \qquad \mathbf{A}_f^c = -\sum_{m_f} \int_{V_f} \mathrm{M}^2 \frac{\partial \mathbf{F}^{\mathrm{T}}}{\partial x}\frac{\partial \mathbf{F}}{\partial x}\, dV,$$

$$\mathbf{C}_f = \sum_{m_\sigma} \int_{S_\sigma} \mathbf{F}^{\mathrm{T}}\mathbf{N}^w\, dS, \qquad \mathbf{C}_f^c = \sum_{m_f} \int_{V_f} \frac{2U}{c^2}\frac{\partial \mathbf{F}^{\mathrm{T}}}{\partial x}\mathbf{F}\, dV.$$

Here, m_f and m_σ are the numbers of finite elements onto which the region of fluid V_f and the plane S_σ are divided; $\mathbf{F}$ and $\mathbf{N}^w$ are the shape functions for the perturbation velocity potential and the normal component w of the plate displacement vector. The fluid volume is discretized by means of a 20-node finite element in the form of a prism with the quadratic approximation of the unknowns [31].

Applying the well-known technique of the finite element method to Eq. (1.12), we obtain

$$\mathbf{K}_s\mathbf{d} + \mathbf{M}_s\ddot{\mathbf{d}} + \mathbf{C}_s\dot{\boldsymbol{\phi}} + \mathbf{A}_s\boldsymbol{\phi} = 0, \tag{2.2}$$

where

$$\mathbf{K}_s = \sum_{m_s} \int_{S_s} \mathbf{B}^{\mathrm{T}}\mathbf{D}\mathbf{B}\, dS, \qquad \mathbf{M}_s = \sum_{m_s} \int_{V_s} \rho_s \mathbf{N}^{\mathrm{T}}\mathbf{N}\, dV,$$

$$\mathbf{C}_s = \sum_{m_\sigma} \int_{S_\sigma} \rho_f \mathbf{F}^{\mathrm{T}}\mathbf{N}^w dS, \qquad \mathbf{A}_s = \sum_{m_\sigma} \int_{S_\sigma} \rho_f U (\mathbf{N}^w)^{\mathrm{T}} \frac{\partial \mathbf{F}}{\partial x} dS.$$

Here, m_s is the number of finite elements onto which the surface of plate is divided; $\mathbf{N}$ are the shape functions of a finite element; and $\mathbf{B}$ is the matrix of relation between the strains and the nodal displacements.

Thus, the problem of investigation of the dynamic behavior of a plate which interacts with flowing fluid reduces to the simultaneous solution of the systems of equations (2.1) and (2.2)

$$\mathbf{M}\{\ddot{\mathbf{d}}\ \ddot{\boldsymbol{\phi}}\}^{\mathrm{T}} + \mathbf{C}\{\dot{\mathbf{d}}\ \dot{\boldsymbol{\phi}}\}^{\mathrm{T}} + (\mathbf{K} + \mathbf{A})\{\mathbf{d}\ \boldsymbol{\phi}\}^{\mathrm{T}} = 0, \tag{2.3}$$

$$\mathbf{K} = \begin{bmatrix} \mathbf{K}_s & 0 \\ 0 & \mathbf{K}_f \end{bmatrix}, \quad \mathbf{M} = \begin{bmatrix} \mathbf{M}_s & 0 \\ 0 & \mathbf{M}_f \end{bmatrix}, \quad \mathbf{C} = \begin{bmatrix} 0 & \mathbf{C}_s \\ -\mathbf{C}_f & \mathbf{C}_f^c \end{bmatrix}, \quad \mathbf{A} = \begin{bmatrix} 0 & \mathbf{A}_s \\ -\mathbf{A}_f & \mathbf{A}_f^c \end{bmatrix}.$$

Here, $\mathbf{K}$, $\mathbf{M}$, $\mathbf{C}$, and $\mathbf{A}$ are the stiffness, mass, damping, and hydrodynamic stiffness matrices, respectively.

We will consider a disturbed motion of the plate and fluid in the following form: $\mathbf{d} = \mathbf{q}\exp(\lambda t)$, $\boldsymbol{\phi} = \mathbf{f}\exp(\lambda t)$, where $\mathbf{q}$ and $\mathbf{f}$ are certain functions of the coordinates and $\lambda = \delta + i\omega$ is the characteristic exponent. Then the system of equations (2.3) can be transformed to the generalized eigenvalue problem for asymmetric matrices of the double dimension

$$\begin{bmatrix} \mathbf{C} & \mathbf{K} \\ -\mathbf{I} & 0 \end{bmatrix} \begin{Bmatrix} \lambda\mathbf{x} \\ \mathbf{x} \end{Bmatrix} + \lambda \begin{bmatrix} \mathbf{M} & 0 \\ 0 & \mathbf{I} \end{bmatrix} \begin{Bmatrix} \lambda\mathbf{x} \\ \mathbf{x} \end{Bmatrix} = 0, \tag{2.4}$$

where $\mathbf{I}$ is a unit matrix and $\mathbf{x} = \{\mathbf{q}\ \mathbf{f}\}^{\mathrm{T}}$. To calculate complex eigenvalues of the problem (2.4) we used the ARPACK procedures based on the implicitly restarted Arnoldi method [32]. The stability criterion is based on an analysis of the roots of Eq. (2.4) obtained for increasing flow velocity [2]. Vibrations damp when $\delta < 0$ and grow when $\delta > 0$, and the dynamic loss of stability in the form of flutter arises. Divergence arises at the frequency $\omega = 0$ and positive δ.

3. RESULTS

The numerical calculations were carried out for the following geometric dimensions and physico-mechanical characteristics: $a = 0.24$ m, $b = 0.32$ m, $h = 2 \times 10^{-3}$ m, $H = 4 \times 10^{-2}$ m, $E = 69$ GPa, $\nu = 0.3$, $\rho_s = 2700$ kg/m^3, $\rho_f = 1000$ kg/m^3, and $c = 1500$ m/s. For representation of the results we use the dimensionless eigenvalue Λ and the dimensionless velocity Υ

$$\Lambda = \Lambda_{\mathrm{Re}} + i\Lambda_{\mathrm{Im}} = a^2\sqrt{\frac{\rho_s h}{D}}\,\lambda, \qquad \Upsilon = a\sqrt{\frac{\rho_s h}{D}}U, \qquad D = \frac{Eh^3}{12(1-\nu^2)}.$$

For the kinematic boundary conditions specified at the plate edges we introduce the following notation: F corresponds to the free edge and C to the rigid clamping ($u = v = w = \theta_x = \theta_y = 0$). In indication of a given combination of boundary conditions the enumeration is carried out clockwise starting from the left edge. For example, the variant CFFF corresponds to a cantilever plate clamped only at the left edge.

The fluid region is discretized taking the compatibility of finite-element meshes on the boundary between two media into account. The subdivision parameters are determined from the condition of analysis of the asymptotic behavior when the number of nodal unknowns increases. In the numerical experiments it was established that the acceptable accuracy of calculations can be reached when the coupled system has approximately 22,000 degrees of freedom. The reliability of the results obtained within the framework of the numerical algorithm developed was tested on the problem of natural vibrations of a plate located in the vacuum and on the layer of quiescent fluid and rigidly clamped at all the edges.

In Table 1 we have given the values of the vibration eigenfrequencies (in Hz) in comparison with the data obtained in [33] and with the use the commercial finite element ANSYS software. Here, n and m denote the number of nodal lines in the directions of the Oy and Ox axes. On all the sides of the rigid container which bounds the fluid we specified the boundary conditions (1.8) or (1.6). In Table 1 the corresponding variants of calculations are denoted by I and II, respectively. The characteristic feature of the latter is the existence of "mixed" vibration shapes which cannot be classified in accordance with the number of rectilinear nodal lines. Thus, the boundary conditions specified in the fluid region affect formation of the vibration shapes. However, in neglecting the combination of wavenumbers to which each of the frequencies corresponds, their effect on the frequency spectrum manifests itself considerably only at low frequencies. In particular, the difference between the first seven frequencies $\omega_1 - \omega_7$ of the spectra I and II reaches 25%, while for the others it does not greater than 10%.

The kinematic boundary conditions specified at the edges of the elastic structure interacting with fluid flow affect significantly the dynamic behavior of the system. The presence of the free edge on the outlet flow side leads to appearance of damping in the system. As a result, the form of the loss of stability can change. In [2, 35, 38] a similar phenomenon was analyzed with reference to circular cylindric shells. In Fig. 2 we have reproduced the typical dependences for plates for two variants of fastening CCCC and CFFF. In this figure we have reproduced the graphs of variation in the real and imaginary parts of the dimensionless eigenvalues Λ for several lowest vibration modes as functions of the dimensionless velocity Υ. As the fluid flow velocity increases, the imaginary part of the second eigenvalue Λ_2 of the plate rigidly clamped at all the edges decreases until it becomes equal to zero at the point Υ_D (Fig. 2a). At this instant the pair of the real parts of this mode appears. With the further variation in the flow velocity the real parts form a characteristic figure in the form of an oval. We note that one of the real parts of the second mode is positive. This corresponds to the static loss of stability in the form of divergence. The further increase in the flow velocity leads subsequently to the divergent instability with respect to the first mode, repeated stabilization for it, and the onset of the secondary instability in the form of coupled flutter [2] achieved as a result of merging two vibration modes when $\Upsilon = \Upsilon_F$: the imaginary parts of the first and fourth modes become identical, a positive real part appearing for each of them. We note that the data on the secondary loss of stability given in Fig. 2 are mainly illustrative. They are represented as an example which clearly demonstrates various forms of the loss of stability and criteria from which the conclusion on their onset is made. In the general case the phenomenon of secondary instability must be analyzed in the nonlinear formulation.

Table 1. Comparison of the vibration eigenfrequencies (Hz) of a plate in the vacuum and on the layer of quiescent fluid

n	m	In the vacuum		On the layer of quiescent fluid		
		[33]	Authors	ANSYS	Authors, I	Authors, II
0	0	243.4	242.32	89.30	89.30	—
	1	409.1	407.17	158.04	158.04	79.39
	2	681.3	680.77	282.27	282.27	195.45
	3	1053	1058.51	470.15	470.15	369.80
1	0	573.3	573.34	230.21	230.21	137.68
	1	726.9	724.74	302.17	302.16	214.57
	2	984.2	982.80	431.15	431.13	348.27
	3	1345.5	1348.14	625.04	625.01	538.71
2	0	1074.2	1083.52	478.33	478.33	363.96
	1	1223.5	1228.91	556.75	556.73	461.08
	2	1470.3	1476.45	693.77	693.73	—
	3	1820	1829.95	896.16	896.09	808.07

In the case of another combination of the boundary conditions (Fig. 2b) characteristic figures also arise in the real part when Λ_{Im} vanishes. However, they are completely located in negative half-plane owing to strongly expressed damping properties of the system. Short-term flutter on a single vibration mode occurs when $\Upsilon = \Upsilon_F$ and the real part of the first mode becomes positive in a short interval $\Upsilon = 7.955$–8.230. Then a secondary stability zone follows. Successive increase in the fluid flow velocity leads to the irreversible loss of stability. Initially, the real part of the third mode becomes positive and then this takes place for the second mode. We note that this version of fastening is characterized by complex nonmonotonic variation in the real part of the eigenvalues.

The numerically-analytic investigations with the use of two-dimensional (infinite in one of the directions) plates make it possible to embrace only partially the possible ways of fastening. The three-dimensional implementation makes it possible to eliminate this imperfection. In Fig. 3 we have given quantitative estimates of the critical flow velocity for the most frequently encountered variants of the boundary conditions. In this figure we have also reproduced the shapes of vibrations of an elastic structure obtained for $\Upsilon = \Upsilon_{cr}$. We note that the lower critical velocities are characteristic of the divergent form of instability than of the flutter. An analysis of the eigenvalues of structures with fastenings of the form CCCC, CFCF, and FCFC showed that there is almost no damping in this systems ($\Lambda_{\mathrm{Re}} \approx 0$). For the remaining variants of the boundary conditions damping is present even at the insignificant fluid flow velocity (real part is negative and not equal to zero). These results make it possible to make the following conclusions: the presence of damping has a stabilizing effect and leads to an increase in the critical velocities of the loss of stability; the boundary conditions specified at the plate edges located parallel to the direction of flow have no effect on the form of instability. We also note that for the plate with the version FCCC of the boundary conditions instability manifests itself at arbitrary low fluid flow velocities. This means that there exist positive real pats of several eigenvalues of the system (2.4). Earlier, a similar phenomenon was revealed for cylindrical shells with asymmetric fastening [34].

Information on the specified boundary conditions for fluid is not complete in the above-mentioned studies of the hydroelastic stability of plates. This not only complicates the comparative analysis but also determines one of the possible directions of the numerical experiments. The previous authors' investigations [30, 35] of the hydroelastic stability of cylindrical shells of revolution showed that the boundary conditions (1.8) and (1.7) at the inlet and outlet, respectively, are that combination which ensures detection of the flutter loss of stability observed experimentally. In Fig. 4 we have reproduced the shapes of vibrations, the critical

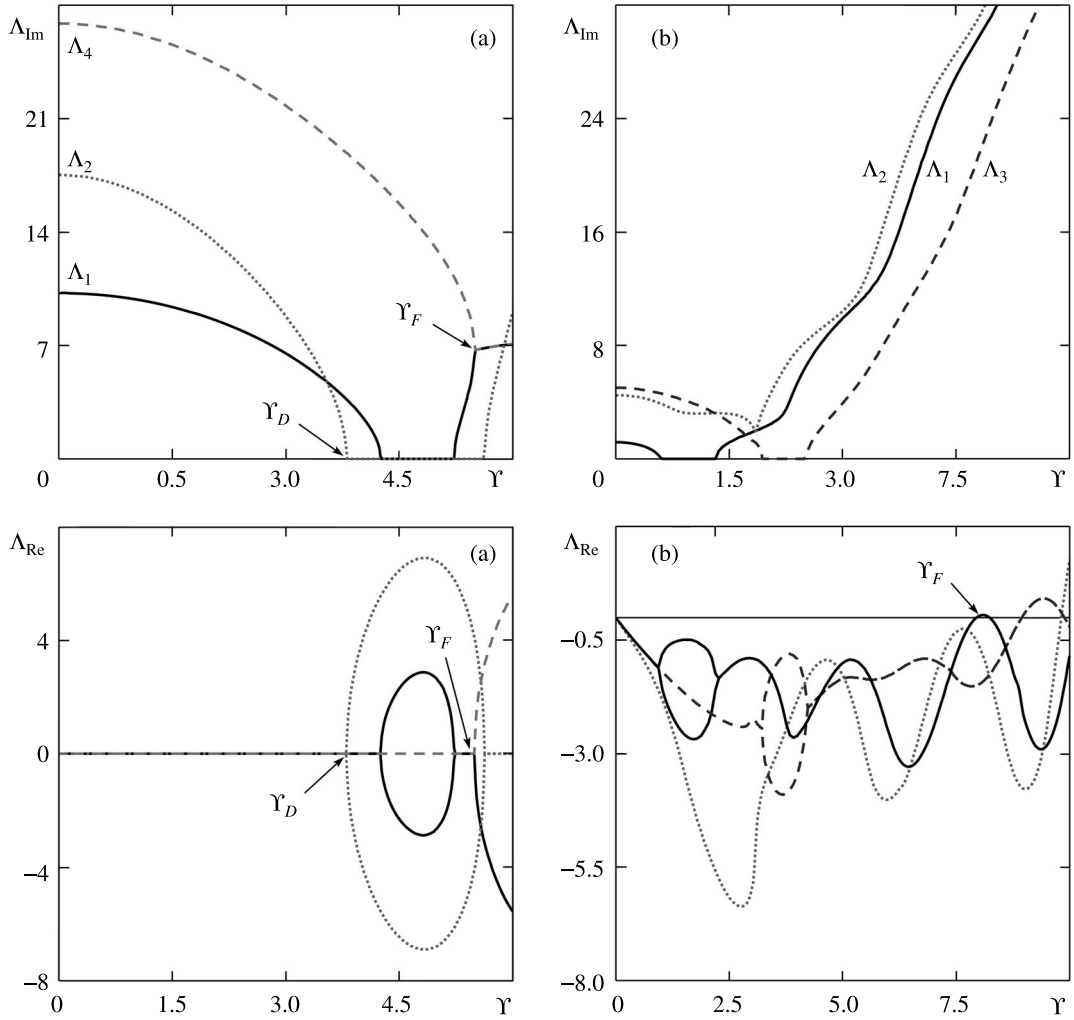

Fig. 2. Variation in the real and imaginary parts of the dimensionless eigenvalues Λ as a function of the dimensionless velocity Υ ($H = 0.05$ m): (a) and (b) correspond to CCCC and CFFF.

velocities, and the form of the loss of stability obtained in this case for plates with similar fastenings. The results demonstrate not only the quantitative but also the qualitative differences. The cantilevered plate flutter sets in at insignificantly higher flow velocities; however, the critical velocities of divergence for fastenings of the form CCCC and FCFC decrease by more than 40%. These variations are due to change in the mode on which the loss of stability is implemented. Despite of the presence of damping ($\delta \neq 0$), the form of instability remains the same for the systems with the boundary conditions CCCC, CFCF, and FCFC.

The fluid layer height H is another factor which affects appreciably the hydroelastic vibrations of the structures considered. When there is no flow ($\Upsilon = 0$), the vibration eigenfrequencies tend to an asymptotic value if the ratio of the characteristic plate dimension to the fluid layer height is greater than unity (see Fig. 5a). This trend is observed for all variants of the boundary conditions given in Fig. 3. Earlier, a similar phenomenon was investigated in [36, 37] for a cantilevered plate totally immersed in water. The asymptotic behavior of the plate vibration eigenfrequencies as functions of the height of fluid layer above the plate was considered on the basis of analytic [36] and finite-element [37] solutions.

In the examples below we will consider the hydroelastic stability of a plate interacting with a fluid flow. In Fig. 5b we have reproduced the graphs of the critical velocity of the loss of stability as a function of the ratio H/b obtained for various variants of fastening. In this example we have used a combination of the boundary conditions (1.7)–(1.7) for fluid. From these data we can see that the asymptotics set in starting

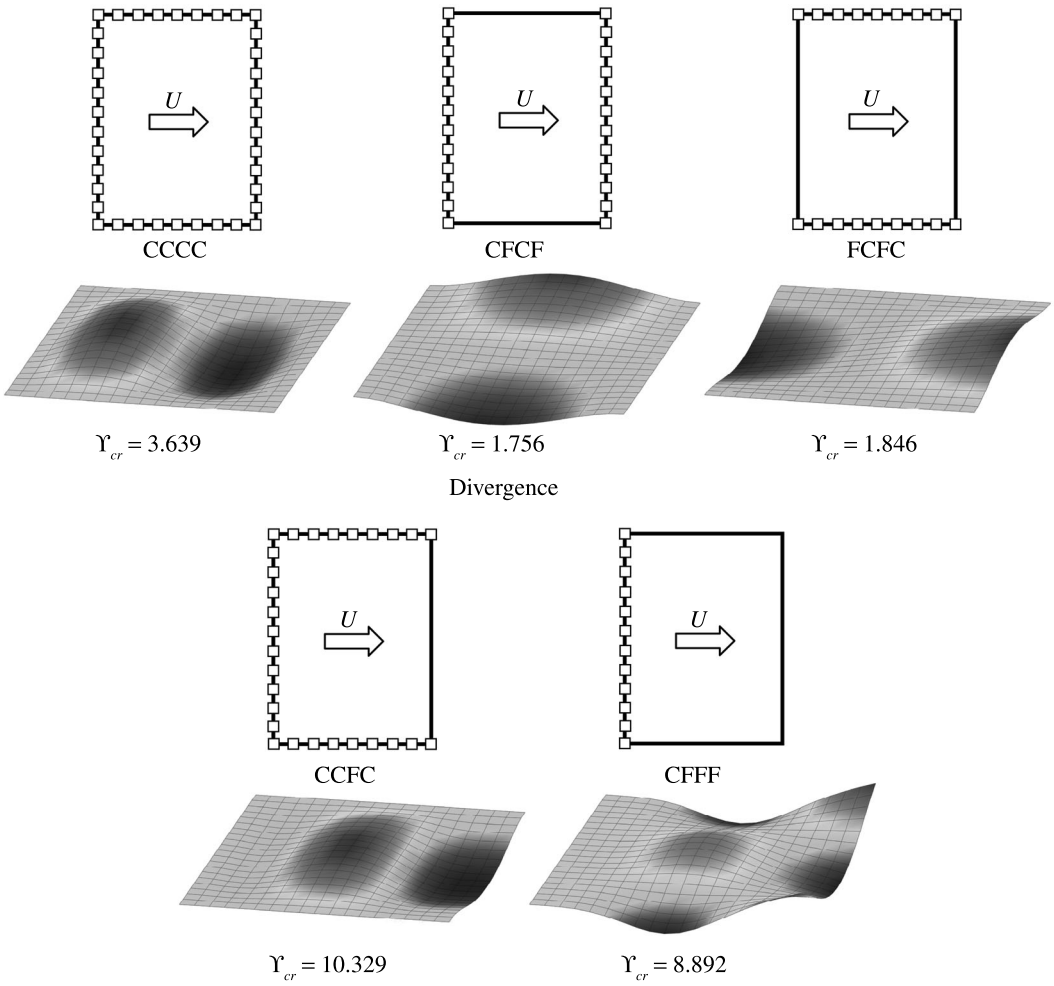

Fig. 3. Shapes of vibrations of a plate under various boundary conditions for $\Upsilon = \Upsilon_{cr}$. The boundary condition (1.7) is specified at the channel inlet.

from $H/b > 0.25$ for the boundary conditions of the form CCCC and CCFC. The curve of critical velocities of the plate restrained along the flow direction on both sides (FCFC) has a point of the local minimum in the neighborhood of $H/b = 0.15$. The successive smooth decrease in the velocity is accompanied by change in the type of the loss of stability from divergence to coupled flutter on two vibration modes. The absence of fastening at the inlet of the structure facilitates not only significant decrease in the critical velocities but also appearance of instability of another form. Curve CFFF corresponding to the cantilevered plate descends sharply when $H/b \approx 0.14$. The cause of this fact is change in the mode on which the loss of stability occurs. In Fig. 2b we have reproduced the data for $H/b = 0.1563$ from which we can see that the first-mode short-term flutter sets in when $\Upsilon = 7.955$–8.230. A detailed analysis showed that the real part of this eigenvalue does not appear in positive half-plane if $H/b < 0.14$. Thus, the system remains stable until the flutter sets in on another mode, in our case this is the second mode. Starting from $H/b \geq 0.14$ a short-term flutter zone develops at the lower flow velocities. This interval of the primary instability expands gradually with increase in the fluid layer height.

In the above models we used the assumption that the fluid volume is bound by the plate dimensions. This assumption not only affects the critical velocities of the loss of stability but also leads to necessity to specify the boundary conditions which can be inconsistent. For example, if the leading edge of the structure is not restrained and the condition (1.8) is specified for fluid at the inlet. In elements of various components of the

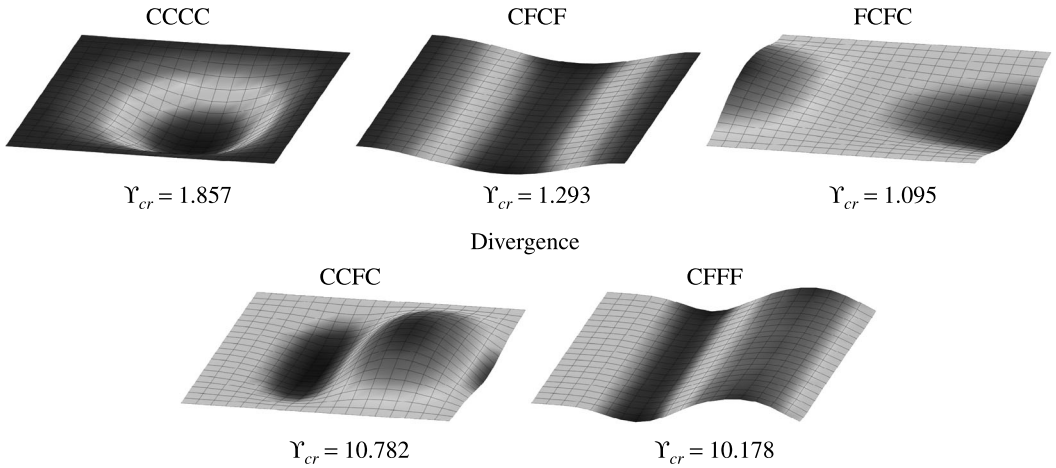

Fig. 4. Shapes of vibrations of a plate under various boundary conditions for $\Upsilon = \Upsilon_{cr}$. The boundary condition (1.8) is specified at the channel inlet.

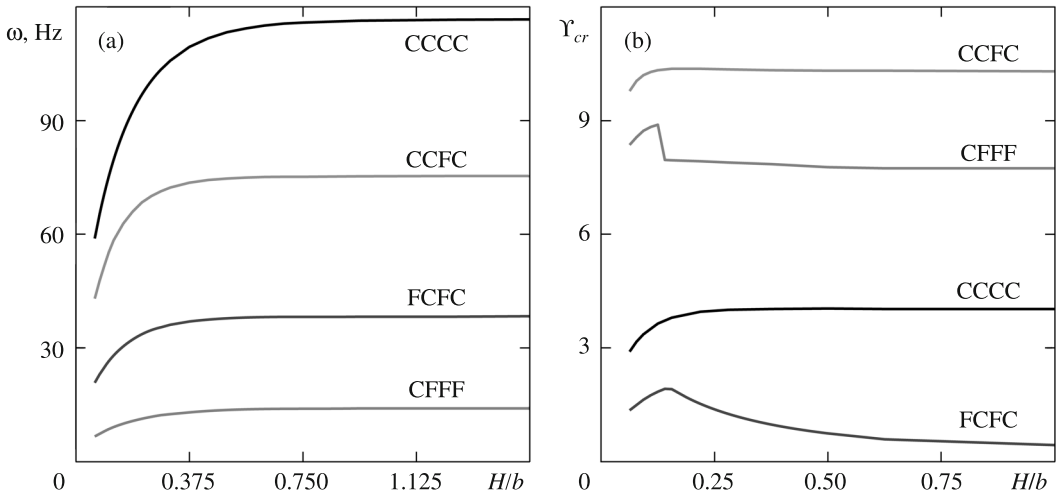

Fig. 5. Lowest vibration eigenfrequencies ω (a) and dimensionless critical velocities Υ (b) as functions of the fluid layer height.

modern atomic power plants and heat exchangers, the channel with rigid walls along which fluid flows can be multiply greater than the dimension of the deformed stream-wise section. A similar structure is simulated in the following example (Fig. 6). The calculations were carried out for two combinations of the boundary conditions for fluid

$$\phi|_{x=0} = \phi|_{x=5a} = 0, \tag{3.1}$$

$$\phi|_{x=0} = 0, \qquad \partial\phi/\partial x|_{x=5a} = 0. \tag{3.2}$$

The condition (3.1) is equivalent to the absence of perturbations far from the plate [25], while the condition (3.2) is considered as an alternative.

In Table 2 we have compared the dimensionless critical velocities of the loss of stability obtained with the use of the first and second computational schemes (Figs. 1 and 6, respectively). An analysis of the results showed that the assumption on boundedness of the fluid volume used above leads to somewhat underestimated critical velocities of divergence and overestimated velocities of flutter. The difference between the values obtained with the use of the boundary conditions (3.1) and (3.2) is insignificant. In both cases the

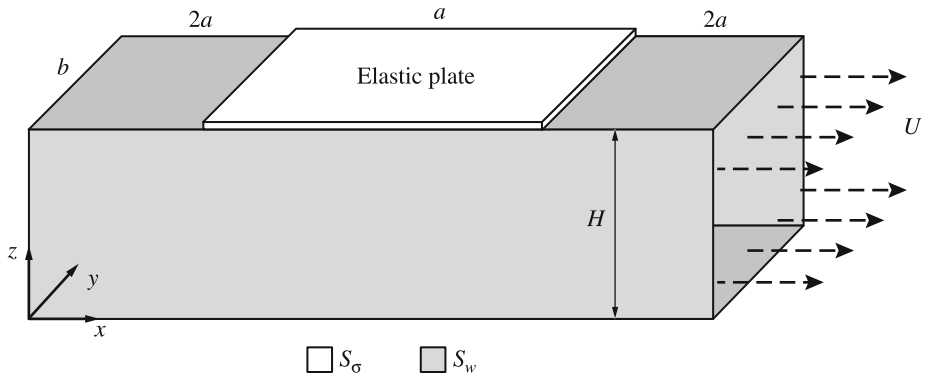

Fig. 6. Computational scheme of the channel whose longitudinal dimension is greater than the plate length.

Table 2. Comparison of the dimensionless critical velocities of the loss of stability

Calculation scheme	Boundary conditions for fluid	Boundary conditions for the plate				
		CCCC	CCFC	FCFC	CFFF	CFCF
Fig. 1	(1.7)–(1.7)	3.639	10.329	1.846	8.892	1.756
	(1.8)–(1.7)	1.857	10.782	1.095	10.178	1.293
Fig. 6	(3.1)	1.969	10.457	1.121	7.228	1.381
	(3.2)	1.857	10.452	—	7.207	1.293

shapes of vibrations correspond to those shown in Fig. 4. An exception is the plate restrained along the direction of flow on two opposite sides (FCFC). In this case instability manifests itself at arbitrary low fluid flow velocities for the boundary conditions of the form (3.2).

Summary. The three-dimensional formulation and the finite element algorithm of its numerical implementation intended for solving the problems on the natural vibrations and stability of an elastic plate which interacts with flowing fluid are presented. The results of computational experiments make it possible to establish existence of various forms of the loss of stability which are determined by the kinematic boundary conditions specified at the plate edges. The data obtained demonstrate the qualitative coincidence with the well-known numerical-analytic solutions.

It is found that the critical velocities of the loss of stability of a plate tend to an asymptotic value (except for several variants of fastening), if the ratio of the characteristic plate dimension to the fluid layer height is greater than $H/b = 0.25$.

It is established that the assumption on boundedness of the fluid volume in accordance with the plate dimensions leads to underestimated values of the critical velocities of divergence and overestimated velocities of flutter.

The work was carried out with support from the Russian Foundation for Basic Research (project No. 15-01-05254) and the Russian Federation President's grant for the state support of young PhD scientists (project No. MK-6167.2015.1).

REFERENCES

1. Yu.N Novichkov, "Flutter of Plates and Shells" in: *Advances of Science and Technology. Mechanics of Deformed Solid Body*, Vol. 11 (VINITI, Moscow, 1978), pp. 67–122.
2. M. P. Païdoussis, *Fluid-Structure Interactions: Slender Structures and Axial Flow*, Vol. 2 (Academic Press, London, 2003).
3. A. Kornecki, E. H. Dowell, and J. O'Brien, "On the Aeroelastic Instability of Two-Dimensional Panels in Uniform Incompressible Flow," J. Sound Vib. **47**, No. 2, 163–178, DOI: 10.1016/0022-460X(76)90715-X (1976).

4. A. Kornecki, "Aeroelastic and Hydroelastic Instabilities of Infinitely Long Plates. II," Solid Mech. Arch. **4**, No. 4, 241–346 (1979).
5. D. M. Minasyan and M. M. Minasyan, "New Approximation in the Problem on Plate Flutter in Supersonic Gas Flow," Dokl. NAN Resp. Armenia **101**, No. 1, 49–54 (2001).
6. V. V. Vedeneev, "Instability of an Unbounded Elastic Plate in a Gas Flow," Fluid Dynamics **39** (4), 526–533 (2004).
7. V. V. Vedeneev, "Flutter of a Wide Strip Plate in a Supersonic Gas Flow," Fluid Dynamics **40** (5), 805–817 (2005).
8. V. V. Vedeneev, "High-Frequency Plate Flutter," Fluid Dynamics **41** (2), 313–321 (2006).
9. D. S. Weaver and T. E. Unny, "The Hydroelastic Stability of a Flat Plate," J. Appl. Mech.-Trans. ASME **37**, No. 3, 823–827, DOI: 10.1115/1.3408615 (1970).
10. Y. Matsuzaki and T. Ueda, "Reexamination of Unsteady Fluid Dynamic Forces on a Two-Dimensional Finite Plate at Small Mach Numbers," J. Appl. Mech. **47**, No. 4, 720–724, DOI: 10.1115/1.3153780 (1980).
11. L. Huang, "Flutter of Cantilevered Plates in Axial Flow," J. Fluids Struct. **9**, No. 2, 127–147, DOI: 10.1006/jfls.1995.1007 (1995).
12. L. Tang and M. P. Païdoussis, "On the Instability and the Post-Critical Behaviour of Two-Dimensional Cantilevered Flexible Plates in Axial Flow," J. Sound Vib. **305**, Nos. 1–2, 97–115, DOI: 10.1016/j.jsv.2007.03.042 (2007).
13. L. Huang and C. Zhang, "Modal Analysis of Cantilever Plate Flutter," J. Fluids Struct. **38**, 273–289, DOI: 10.1016/j.jfluidstructs.2013.01.004 (2013).
14. C. H. Ellen, "The Stability of Simply Supported Rectangular Surfaces in Uniform Subsonic Flow," J. Appl. Mech. **40**, No. 1, 68–72, DOI: 10.1115/1.3422974 (1973).
15. C. H. Ellen, "The Stability of an Isolated Rectangular Surface Embedded in Uniform Subsonic Flow," J. Appl. Mech. **44**, No. 2, 201–206, DOI: 10.1115/1.3424024 (1977).
16. L. K. Shayo, "The Stability of Cantilever Panels in Uniform Incompressible Flow," J. Sound Vib. **68**, No. 3, 341–350, DOI: 10.1016/0022-460X(80)90391-0 (1980).
17. A. D. Lucey and P. W. Carpenter, "The Hydroelastic Stability of Three-Dimensional Disturbances of a Finite Compliant Wall," J. Sound Vib. **165**, No. 3, 527–552, DOI: 10.1006/jsvi.1993.1275 (1993).
18. M. Argentina and L. Mahadevan, "Fluid-Flow-Induced Flutter of a Flag," PNAS **102**, No. 6, 1829–1834, DOI: 10.1073/pnas.0408383102 (2005).
19. C. Eloy, C. Souilliez, and L. Schouveiler, "Flutter of a Rectangular Plate," J. Fluids Struct. **23**, No. 6, 904–919, DOI: 10.1016/j.jfluidstructs.2007.02.002 (2007).
20. C. Q. Guo and M. P. Païdoussis, "Stability of Rectangular Plates with Free Side-Edges in Two-Dimensional Inviscid Channel Flow," J. Appl. Mech. **67**, No. 1, 171–176, DOI: 10.1115/1.321143 (1999).
21. R. M. Howell, A. D. Lucey, P. W. Carpenter, and M. W. Pitman, "Interaction between a Cantilevered-Free Flexible Plate and Ideal Flow," J. Fluids Struct. **25**, No. 3, 544–566, DOI: 10.1016/j.jfluidstructs.2008.12.004 (2009).
22. O. Doare, M. Sauzade, and C. Eloy, "Flutter of an Elastic Plate in a Channel Flow: Confinement and Finite-Size Effects," J. Fluids Struct. **27**, No. 1, 76–88, DOI: 10.1016/j.jfluidstructs.2010.09.002 (2011).
23. X. Wu and S. Kaneko, "Linear and Nonlinear Analyses of Sheet Flutter Induced by Leakage Flow," J. Fluids Struct. **20**, No. 7, 927–948, DOI: 10.1016/j.jfluidstructs.2005.05.008 (2005).
24. T. Balint and A. D. Lucey, "Instability of a Cantilevered Flexible Plate in Viscous Channel Flow," J. Fluids Struct. **20**, No. 7, 893–912, DOI: 10.1016/j.jfluidstructs.2005.05.005 (2005).
25. Y. Kerboua, A. A. Lakis, M. Thomas, and L. Marcouiller, "Modeling of Plates Subjected to a Flowing Fluid under Various Boundary Conditions," Eng. Appl. Comp. Fluid Mech. **2**, No. 4, 525–539, DOI: 10.1080/19942060.2008.11015249 (2008).
26. M. A. Il'gamov, *Vibrations of Elastic Shells Containing Liquid and Gas* (Nauka, Moscow, 1969) [in Russian].
27. V. V. Mokeyev, "On a Method for Vibration Analysis of Viscous Compressible Fluid-Structure Systems," Int. J. Numer. Methods Eng. No. 13, 1703–1723, DOI: 10.1002/nme.930 (2004).
28. M. A. Langthjem and N. Olhoff, "Modal Expansion of the Perturbation Velocity Potential for a Cantilevered Fluid-Conveying Cylindrical Shell," J. Fluids Struct. **17**, No. 1, 147–161, DOI: 10.1016/S0889-9746(02)00113-5 (2003).
29. A. S. Vol'mir, *Nonlinear Dynamics of Plates and Shells* (Nauka, Moscow, 1972) [in Russian].

30. S. A. Bochkarev and V. P. Matveenko, "Numerical Investigation of the Effect of Boundary Conditions on Dynamics of the Behavior of a Cylindrical Shell with Flowing Fluid," Izvestiya RAN, Mechanics of Solid Body, No. 3, 189–199 (2008).
31. O. C. Zienkiewicz, *Finite Element Method in Engineering Science* (McGraw-Hill, New York, 1972).
32. R. B. Lehoucq and D. C. Sorensen, "Deflation Techniques for an Implicitly Restarted Arnoldi Iteration," SIAM J. Matrix Anal. Appl. **17**, No. 4, 789–821, DOI: 10.1137/S0895479895281484 (1996).
33. K.-H. Jeong, G.-H. Yoo, and S.-C. Lee, "Hydroelastic Vibration of Two Identical Rectangular Plates," J. Sound Vib. **272**, Nos. 3–5, 539–555, DOI: 10.1016/S0022-460X(03)00383-3 (2004).
34. J. Horaček and I. Zolotarev, "Influence of Fixing the Edges of a Cylindrical Shell with Conveying Fluid on its Dynamic Characteristics," Int. J. Appl. Mech. **20**, No. 8, 756–765, DOI: 10.1007/BF00889459 (1984).
35. S. A. Bochkarev and V. P. Matveenko, "Natural Vibrations and Stability of Shells of Revolution Interacting with an Internal Fluid Flow," J. Sound Vib. **330**, No. 13, 3084–3101, DOI: 10.1016/j.jsv.2011.01.029 (2011).
36. Y. Fu and W. G. Price, "Interactions between a Partially or Totally Immersed Vibrating Cantilever Plate and the Surrounding Fluid," J. Sound Vib. **118**, No. 3, 495–513, DOI: 10.1016/0022-460X(87)90366-X (1987).
37. Y. Kerboua, A. A. Lakis, M. Thomas, and L. Marcouiller, "Vibration Analysis of Rectangular Plates Coupled with Fluid," Appl. Math. Model **32**, No. 12, 2570–2586, DOI: 10.1016/j.apm.2007.09.004 (2008).